

On mode-1 and mode-2 internal solitary waves in a three-layer fluid system

T.Y. Zhang¹, Z. Wang¹, Z.H. Wang¹, B.T. Xie², B.B. Zhao^{1,*}, W.Y. Duan¹, M. Hayatdavoodi^{1,3}

¹ College of Shipbuilding Engineering, Harbin Engineering University, Harbin, China

² CNOOC Research Institute CO., Ltd

³ Civil Engineering Department, School of Science and Engineer, University of Dundee, Dundee, UK

*zhaobinbinheu@hotmail.com

Highlights:

- Experiments are conducted on the mode-1 and mode-2 internal solitary waves in strong density stratification for a three-layer fluid system with free surface.
- High-Level Green-Naghdi (HLGN) equations are used to study this problem.
- Results of the HLGN equations are compare with the laboratory experiments, and with other available data.
- Results of the HLGN equations are compare with the field data of South China Sea.

1 Introduction

Internal solitary waves, which occur in the interior of ocean due to differences in density between adjacent layers of water (stratification), have been observed frequently in lakes, coastal areas and continental shelf regions, see e.g. Helfrich and Melville (2006) and Shroyer et al. (2010). In the study of internal solitary waves, there is always a two-layer or three-layer fluid system.

For internal solitary waves in a two-layer fluid system, Grue et al. (1999) investigated the internal solitary-wave profile and velocity field experimentally and numerically, and good agreement was observed. Zhao et al. (2016) derived the two-layer strongly nonlinear, strongly dispersive wave model, namely the High-Level Green-Naghdi (HLGN) model, to study the internal solitary waves. Zhao et al. (2016) showed that the HLGN results matched well with Euler's solution of Grue et al. (1999).

In a three-layer fluid system, the mode-1 internal solitary wave is defined when the isopycnals is displaced in the same direction as the wave. Mode-2 internal waves, however, refers to when the isopycnals is displaced in the opposite direction. There are some experimental studies on mode-2 internal solitary waves, see e.g. Carr et al. (2015). For the theoretical investigations and numerical analysis, Barros et al. (2020) developed a strongly nonlinear long-wave model for large-amplitude internal waves in a three-layer fluid system between two rigid boundaries, which can be used to describe the propagation of mode-1 and mode-2 internal solitary waves.

In this study, we focus on the three-layer system with strong density stratification, and calculate the mode-1 and mode-2 internal solitary waves by the High-Level Green-Naghdi model with a free surface (HLGN-FS model). This model is an extension of the two-layer HLGN-FS model recently developed by Wang et al. (2019).

The governing equations of three-layer HLGN-FS model is described in Section 2. Laboratory experiments are discussed in Section 3, along with comparison of the theoretical models. The real-scale numerical study on internal solitary waves in South China Sea is shown in Section 4. Conclusions are presented in Section 5.

2 The governing equations

The sketch of the internal solitary waves in a three-layer system is shown in Fig. 1. All fluids are immiscible and inviscid. The mass densities of the three layers are ρ_1, ρ_2, ρ_3 , and the depths are h_1, h_2, h_3 , from the upper layer to the lower layer, respectively. We set the coordinate origin at the interface between the upper layer and the middle layer before it is disturbed. The free surface, upper interface, lower interface and bottom are expressed by $z = \eta_1(x, t)$, $z = \eta_2(x, t)$, $z = \eta_3(x, t)$ and $z = -(h_2 + h_3)$, respectively. The equations are given here in two dimensions.

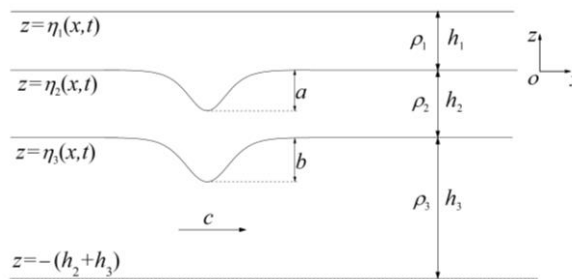


Fig. 1 Sketch of the internal solitary waves in a three-layer fluid system.

The continuity equations are written as

$$\frac{\partial u_i}{\partial x} + \frac{\partial w_i}{\partial z} = 0 \quad (i = 1, 2, 3), \quad (1)$$

where u and w are the horizontal and vertical velocity components, respectively, and index i refers to the fluid layer.

Euler's equations are written as

$$\frac{\partial u_i}{\partial t} + u_i \frac{\partial u_i}{\partial x} + w_i \frac{\partial u_i}{\partial z} = -\frac{1}{\rho_i} \frac{\partial p_i}{\partial x} \quad (i = 1, 2, 3), \quad (2a)$$

$$\frac{\partial w_i}{\partial t} + u_i \frac{\partial w_i}{\partial x} + w_i \frac{\partial w_i}{\partial z} = -\frac{1}{\rho_i} \frac{\partial p_i}{\partial z} - g \quad (i = 1, 2, 3), \quad (2b)$$

where p is pressure and g is the gravitational acceleration.

The kinematic boundary conditions are written as

$$w_1 = \frac{\partial \eta_1}{\partial t} + u_1 \frac{\partial \eta_1}{\partial x} \quad z = \eta_1(x, t), \quad (3a)$$

$$w_{i-1} = \frac{\partial \eta_i}{\partial t} + u_{i-1} \frac{\partial \eta_i}{\partial x}, \quad w_i = \frac{\partial \eta_i}{\partial t} + u_i \frac{\partial \eta_i}{\partial x} \quad (z = \eta_i(x, t), \quad i = 2, 3), \quad (3b)$$

$$w_3 = 0 \quad z = -(h_2 + h_3). \quad (3c)$$

The dynamic boundary conditions are written as

$$\hat{p}_1 = p \Big|_{z=\eta_1(x,t)} = 0 \quad (\text{atmospheric pressure}), \quad (4a)$$

$$\bar{p}_i = \hat{p}_{i+1} = p \Big|_{z=\eta_{i+1}(x,t)} \quad (i = 1, 2). \quad (4b)$$

We use the High-Level Green-Naghdi model to solve this physical problem, where the horizontal and vertical velocities are expressed in polynomial forms for each fluid layer as

$$u_i(x, z, t) = u_{i,0}(x, t) + u_{i,1}(x, t)z + \cdots + u_{i,K-1}(x, t)z^{K-1} \quad (i = 1, 2, 3), \quad (5a)$$

$$w_i(x, z, t) = w_{i,0}(x, t) + w_{i,1}(x, t)z + \cdots + w_{i,K}(x, t)z^K \quad (i = 1, 2, 3), \quad (5b)$$

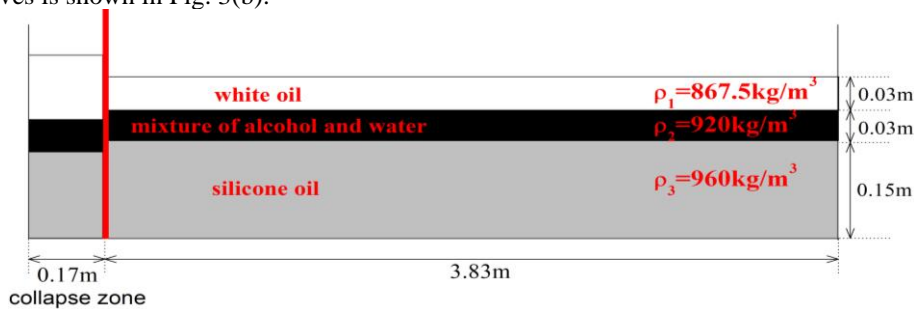
where K is the level of the HLG model. The HLG-FS equations for the three-layer fluid system with free surface are obtained by substituting Eq. (5) into Eqs. (1)-(4). The system of equations of all fluid system is solved simultaneously by using a seven-point difference method for spatial derivatives and by fourth-order Adams predictor-corrector method for time marching.

3 Laboratory experiments and comparisons with theoretical models

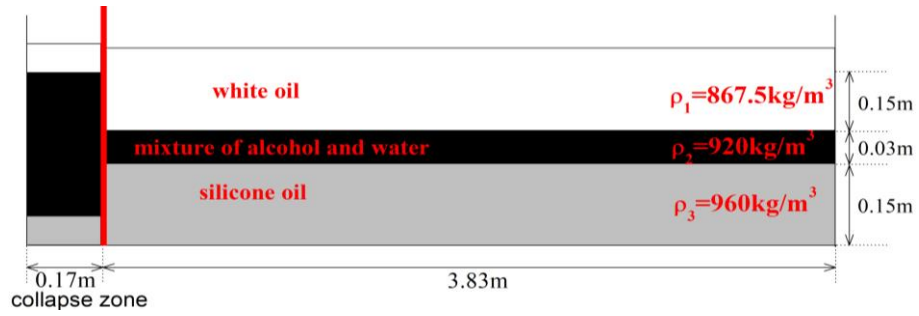
The laboratory experiments are conducted at Harbin Engineering University. Sketches of the experimental set-up of the three-layer mode-1 and mode-2 internal solitary waves are shown in Figs. 2(a) and 2(b), respectively. The mass density of the upper fluid (white oil) is 867.5 kg/m^3 , the mass density of the middle fluid (the mixture of alcohol and fresh water) is 920 kg/m^3 and the lower fluid (silicone oil) is 960 kg/m^3 . We select the gravity collapse method to generate internal solitary waves. A grid plate is used to measure the wave profile.

To generate the mode-1 internal solitary waves, we select the thicknesses of the three layers as 0.03m, 0.03m, 0.15m shown in Fig. 2(a). By changing the thickness of the upper layer in the collapse zone, the mode-1 internal solitary waves with different amplitudes can be generated. A snapshot of the mode-1 internal solitary waves is shown in Fig. 3(a).

To generate the mode-2 internal solitary waves, we select the thicknesses of the three layers as 0.15m, 0.03m, 0.15m shown in Fig. 2(b). By increasing the thickness of the middle layer and decreasing the thickness of the upper layer in the collapse zone, the mode-2 internal solitary waves with different amplitudes can be generated. A snapshot of mode-2 internal solitary waves is shown in Fig. 3(b).



(a) Mode-1 internal solitary wave

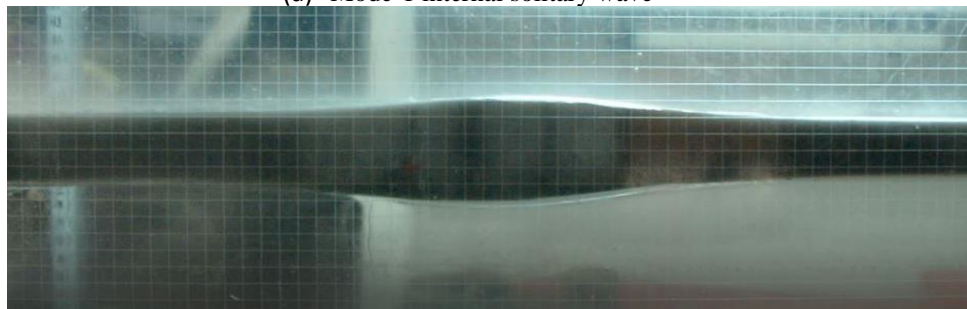


(b) Mode-2 internal solitary wave

Fig.2 Experimental set-up of the three-layer internal solitary waves.



(a) Mode-1 internal solitary wave



(b) Mode-2 internal solitary wave

Fig.3 Snapshots of mode-1 and mode-2 internal solitary waves generated in the laboratory.

For the mode-1 internal solitary wave, we compare the results of the HLGN-FS model developed here, with the results of the KdV model and the strongly nonlinear internal wave model (SNIWM) derived of Barros et al. (2020) with the results of the laboratory experiments conducted here. We note that the rigid-lid approximation is used in the KdV model and the SNIWM. Results are shown in Fig. 4.

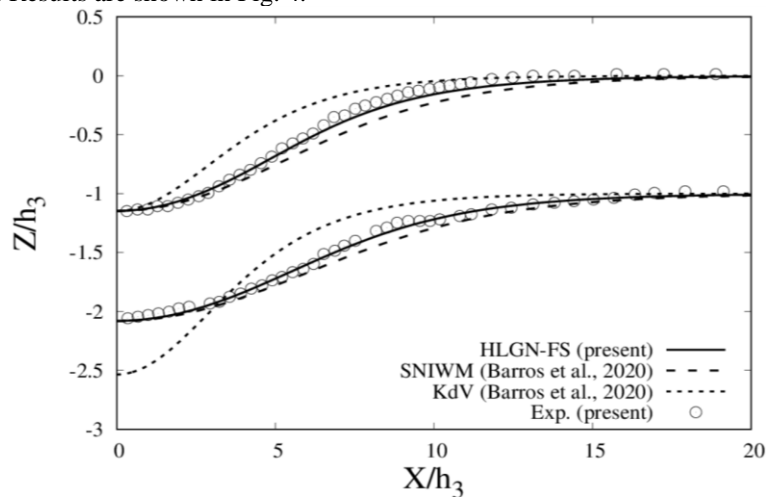


Fig. 4 Profile of mode-1 internal solitary wave, $a/h_3=1.148$.

Shown in Fig. 4, the results of the HLGN-FS model are in good agreement with experimental data. Although the rigid-lid approximation is used in the SNIWM, its results are close to the HLGN-FS results and the laboratory measurements. Meanwhile, the results of the KdV model show some differences with others.

More comparisons between the experimental data and numerical results on mode-1 and mode-2 internal solitary waves will be presented and discussed at the workshop.

4 Real -scale numerical study on internal solitary waves in South China Sea

Field observations of internal solitary waves in South China Sea is shown in Fig. 5. A typical mode-1 internal solitary wave with an amplitude of about 82m is captured by CNOOC Research Institute at 1:00 AM on April 21, 2011.

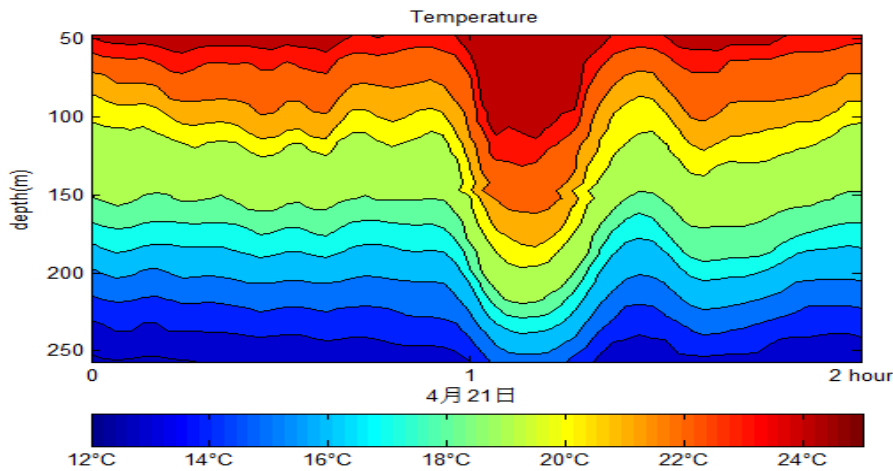


Fig. 5 Mode-1 internal solitary waves in South China Sea.

Results of the comparison between the real-scale mode-1/mode-2 internal solitary waves and the HLGN-FS model results will be presented at the workshop.

5 Conclusions

Internal solitary waves in a three-layer fluid system with a free surface are investigated both experimentally and numerically. For the experiments, we generate the mode-1 and mode-2 internal solitary waves. Good agreement is observed between the experimental data and the HLGN-FS results. The HLGN model is not limited to the laboratory experiments, but also to real-scale ocean observations. It is expected that the HLGN-FS model can be used to describe the real-world internal solitary waves efficiently and accurately.

Acknowledgments

The fifth and sixth authors' (B.B. Zhao and W.Y. Duan) work is supported by the National Natural Science Foundation of China (Nos. 11572093, 11972126, 51490671, 11772099, 5167904), the Heilongjiang Touyan Innovation team Program and the special Fund for Basic Scientific Research of Central Colleges (Harbin Engineering University).

References

- [1] Helfrich, K. R. & Melville, W. K. (2006). Long nonlinear internal waves. *Annu. Rev. Fluid Mech.*, 38, 395-425.
- [2] Shroyer, E. L., Moum, J. N. & Nash, J. D. (2010). Mode 2 waves on the continental shelf: Ephemeral components of the nonlinear internal wavefield. *J. Geophys. Res.*, 115, C07001.
- [3] Grue, J., Jensen, A., Rusås, P. -O., & Svein, J. K. (1999). Properties of large-amplitude internal waves. *J. Fluid Mech.*, 380(2), 257-278.
- [4] Zhao, B. B., Ertekin, R. C., Duan, W. Y., & Webster, W. C. (2016). New internal-wave model in a two-layer Fluid. *J. Waterway, Port, Coastal, Ocean Eng.*, 04015022.
- [5] Carr, M., Davies, P. A. & Hoebbers, R. P. (2015). Experiments on the structure and stability of mode-2 internal solitary-like waves propagating on an offset pycnocline. *Phys. Fluids*, 27, 046602.
- [6] Barros, R., Choi, W., & Milewski, P. A. (2020). Strongly nonlinear effects on internal solitary waves in three-layer flows. *J. Fluid Mech.*, 883, A16.
- [7] Wang, Z., Zhao, B. B., Duan, W. Y. & Zhang, T. Y. (2019). Application of the high-level Green-Naghdi model on internal solitary waves with a free surface. *Proc. 34th IWWFEB, Newcastle (Australia)*.